Supplemental Information: Oxidation of TcO_2 and UO_2 by Aqueous Mn(III)-Citrate and Mn(III)-Tartrate Under Anoxic Conditions: Implications for Technetium and Uranium Fate and Transport

S1. Sample Characterization

XRD (Empyrean, PANalytical) was conducted with a 1.8 KW copper X-ray tube (1.54 A) and measured at a 2θ range of 20˚ to 70˚. The synthesized uraninite was analyzed before and after dissolution and compared to literature.[1, 2] SEM (NVision 40, Zeiss) was used to analyze the UO_2 particle size and morphology before and after dissolution. An In-Lens detector and an acceleration voltage of 15 kV was used for imaging. The hydrodynamic particle size distribution was also analyzed with DLS (Zetasizer ZS90, PANalytical) in disposable cuvettes. ^{1}H-NMR (AvanceIII 500, Bruker) analysis was conducted on a 50 mM Mn(III)-tartrate solution following the same synthesis procedure in D_2O, however substantial manganese precipitation was observed, indicating a solution of less than 50 mM Mn(III)-tartrate.

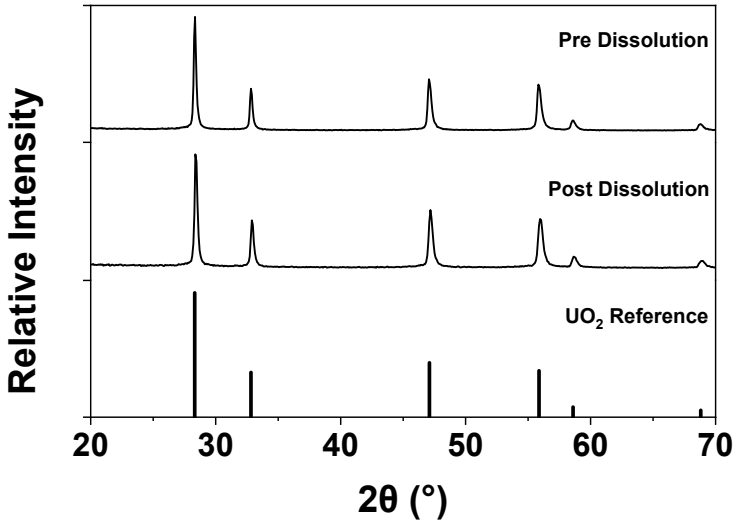

Figure S1. XRD of the UO_2 solid phase before and after dissolution with 3 mM Mn(III)-Tartrate at pH 8. No phase changes after dissolution are observed.

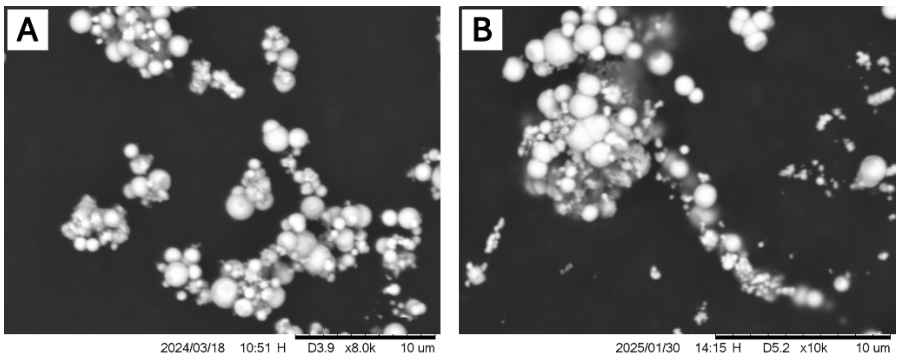

Figure S2. SEM of the UO_2 solid phase before and after dissolution with 3 mM Mn(III)-tartrate at pH 8. Similar particle size and morphology are found before and after dissolution.

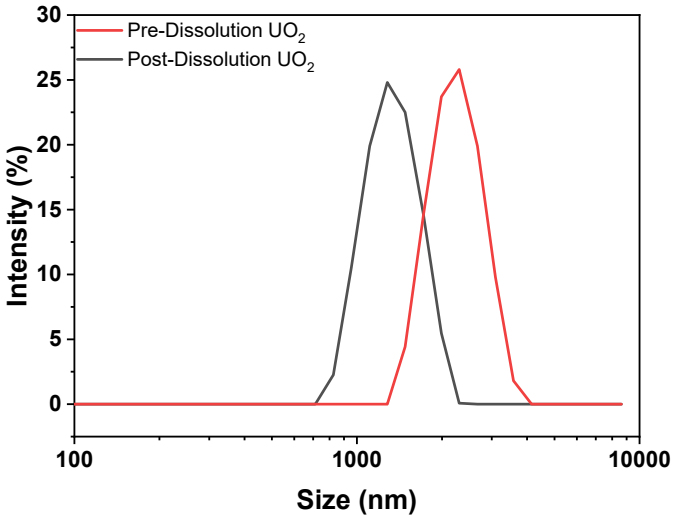

Figure S3. DLS particle size analysis of the UO_2 solid phase before and after dissolution with 3 mM Mn(III)-tartrate at pH 8. Particles before dissolution had an average diameter of 2236 nm with a PDI of 0.074, while particles after dissolution had an average diameter of 1452 nm with a PDI of 0.134.

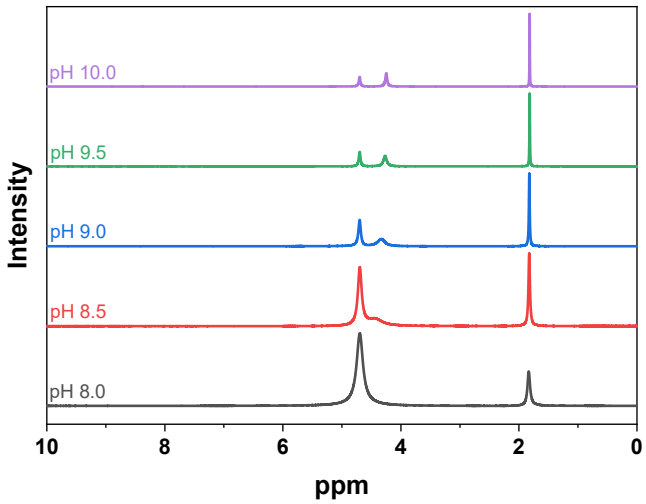

Figure S4. ^{1}H-NMR of <50 mM Mn(III)-tartrate, 250 mM tartrate, and 50 mM acetate in D_2O at pH 8.0 (gray), pH 8.5 (red), pH 9.0 (blue), pH 9.5 (green), and pH 10.0 (purple). Acetate is present from the initial Mn(III) acetate stock used in synthesis.

S2. Pourbaix Diagrams

Pourbaix diagrams were constructed using free Hydra-Medusa software. The relevant parameters used to construct the diagrams are summarized in Table S1. Free ligands (citrate or tartrate) were not included in these diagrams but could contribute to uranium speciation from ligand complexation.

Table S1. Pourbaix diagram parameters

Parameter	Setting
[U]	1.85 mM
[Tc]	0.15 mM
$[CO_3^{2-}]$	15.8 mM
Temperature	298 K

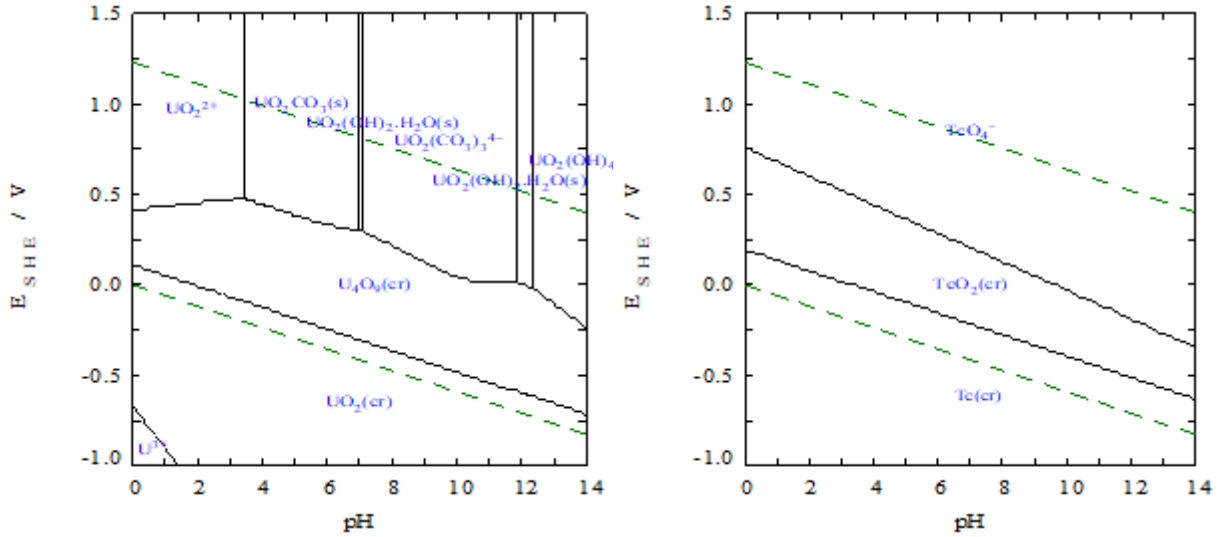

Figure S5. Pourbaix diagrams of uranium (left) and technetium (right). Relevant parameters are summarized in Table S1.

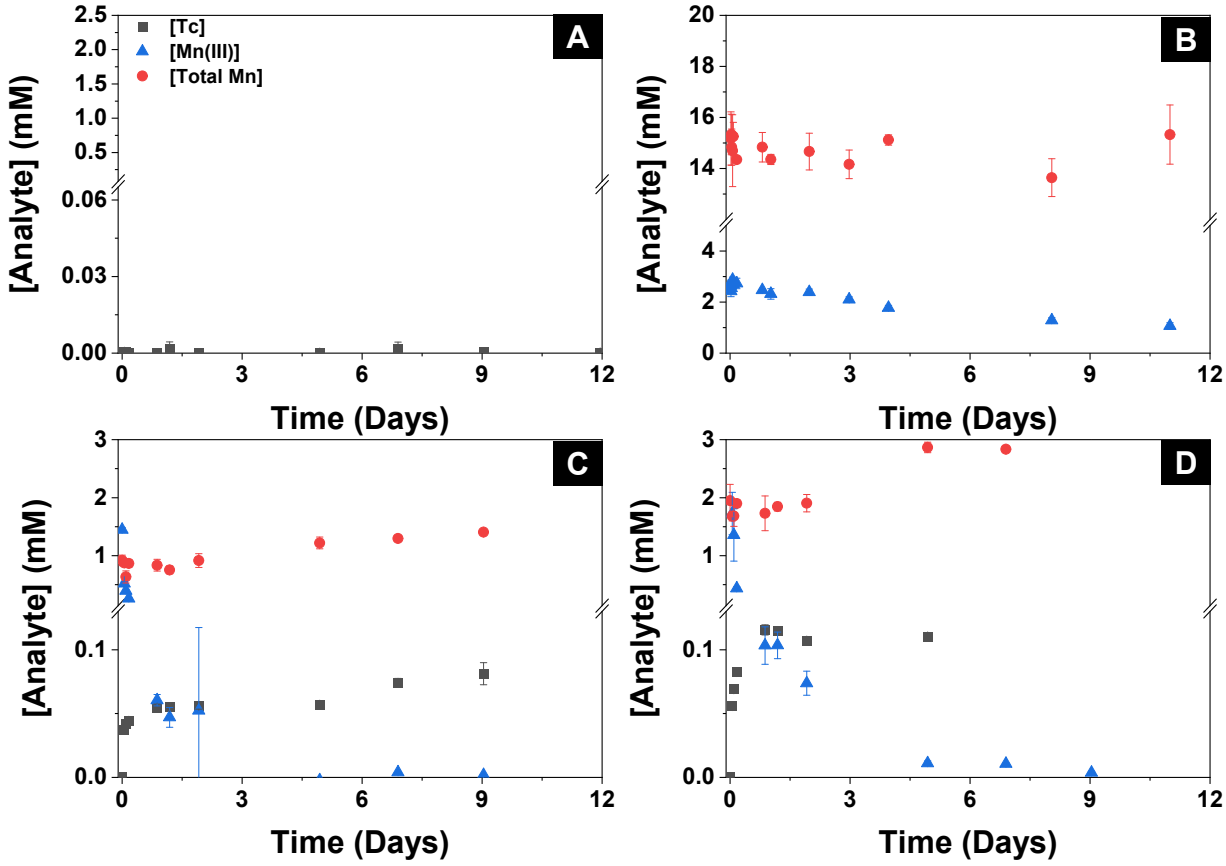

Figure S6. Dissolution trials at pH 8 of (A) TcO_2 in 250 mM tartrate, (B) Mn(III)-tartrate in the absence of TcO_2, (C) TcO_2 in 1.5 mM Mn(III)-tartrate, and (D) TcO_2 in 3 mM Mn(III)-tartrate.

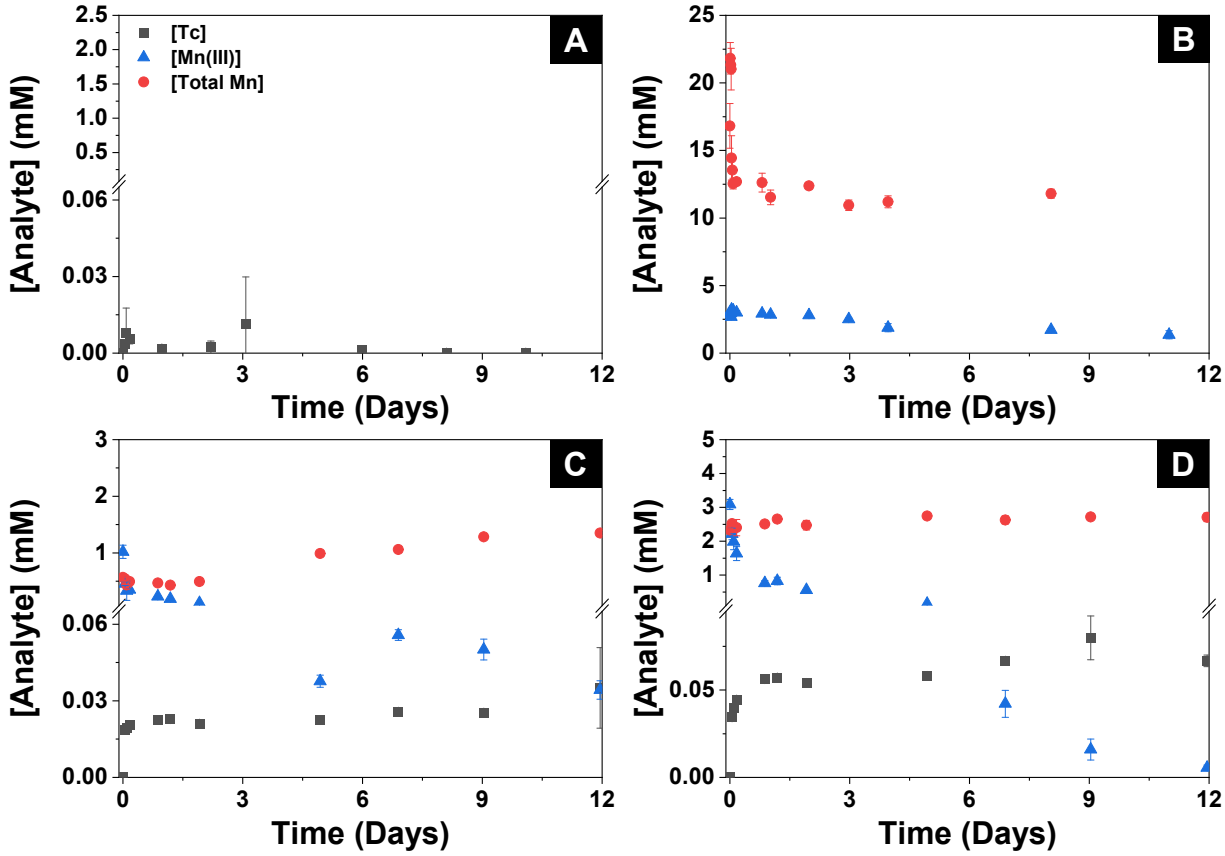

Figure S7. Dissolution trials at pH 10 of (A) TcO_2 in 250 mM tartrate, (B) Mn(III)-tartrate in the absence of TcO_2, (C) TcO_2 in 1.5 mM Mn(III)-tartrate, and (D) TcO_2 in 3 mM Mn(III)-tartrate.

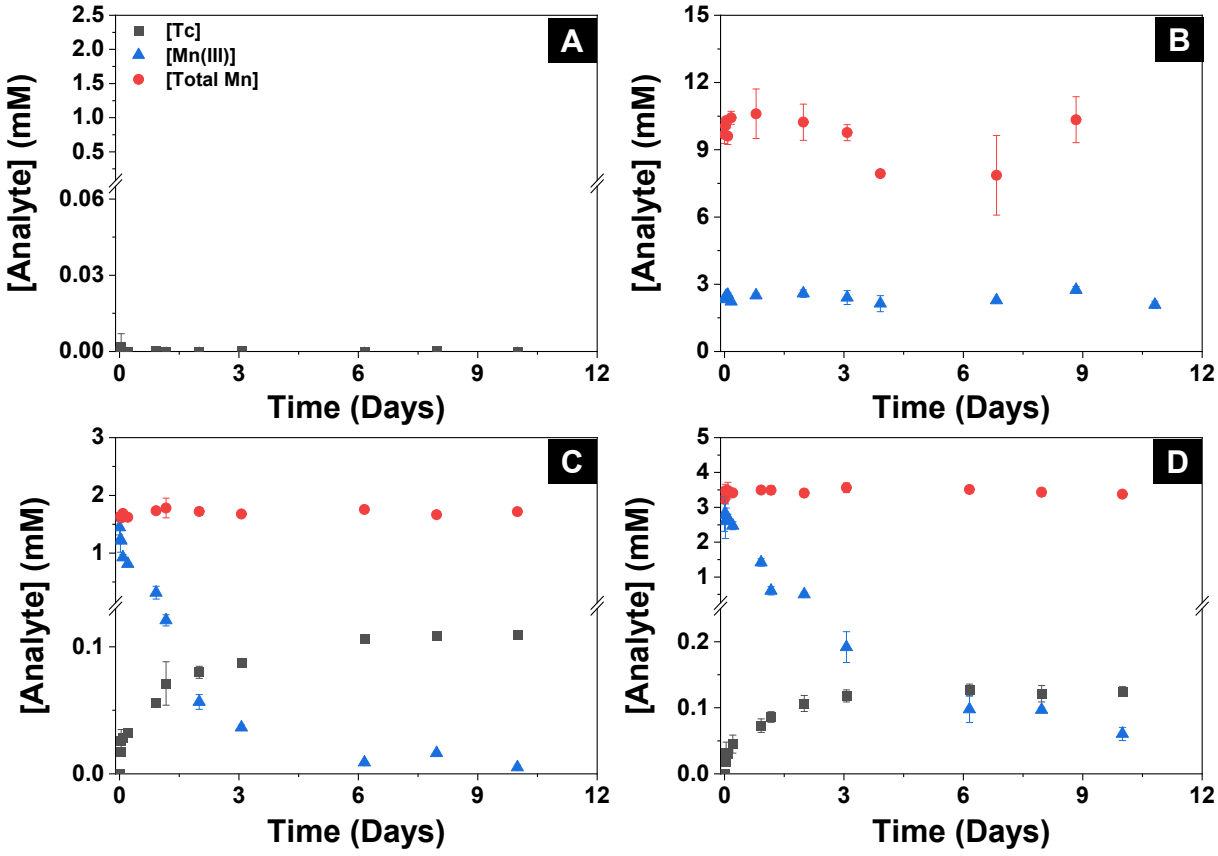

Figure S8. Dissolution trials at pH 8 of (A) TcO_2 in 250 mM citrate, (B) Mn(III)-citrate in the absence of TcO_2, (C) TcO_2 in 1.5 mM Mn(III)-citrate, and (D) TcO_2 in 3 mM Mn(III)-citrate.

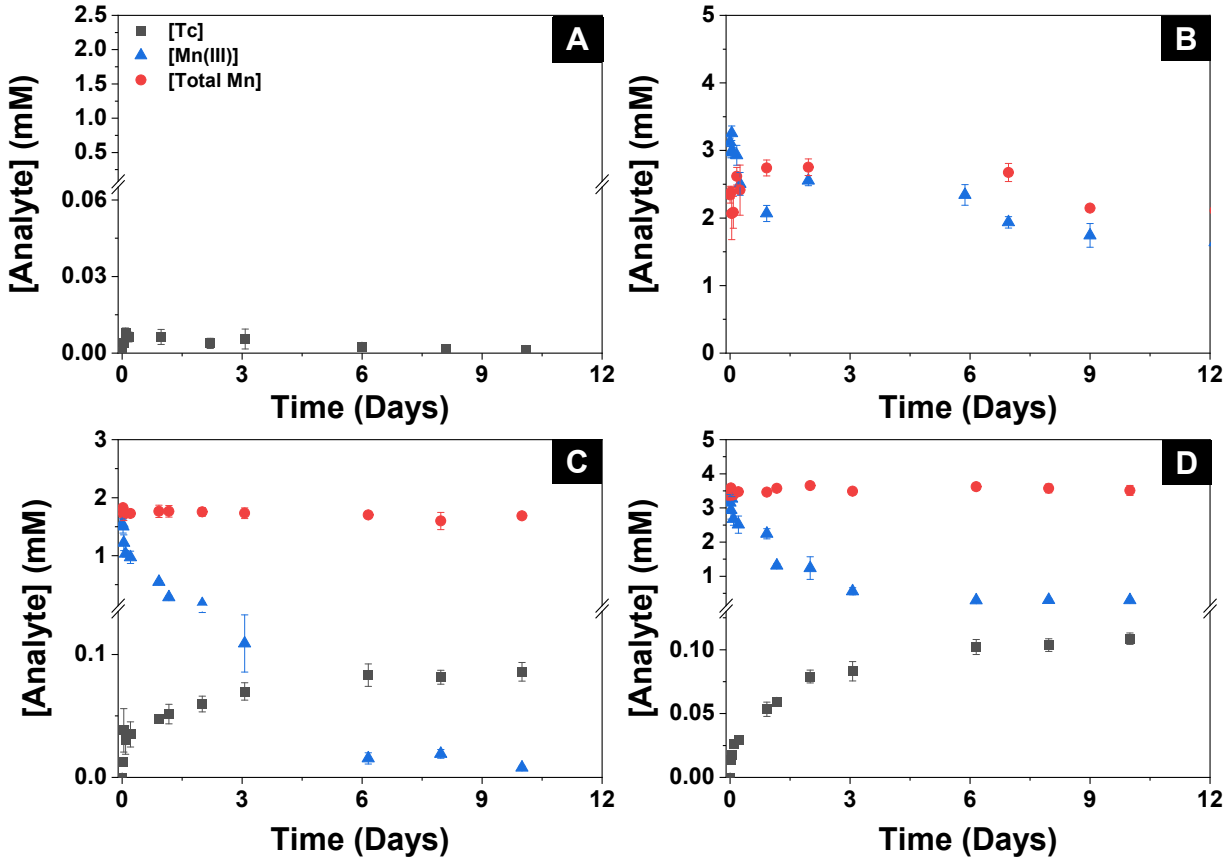

Figure S9. Dissolution trials at pH 10 of (A) TcO_2 in 250 mM citrate, (B) Mn(III)-citrate in the absence of TcO_2, (C) TcO_2 in 1.5 mM Mn(III)-citrate, and (D) TcO_2 in 3 mM Mn(III)-citrate.

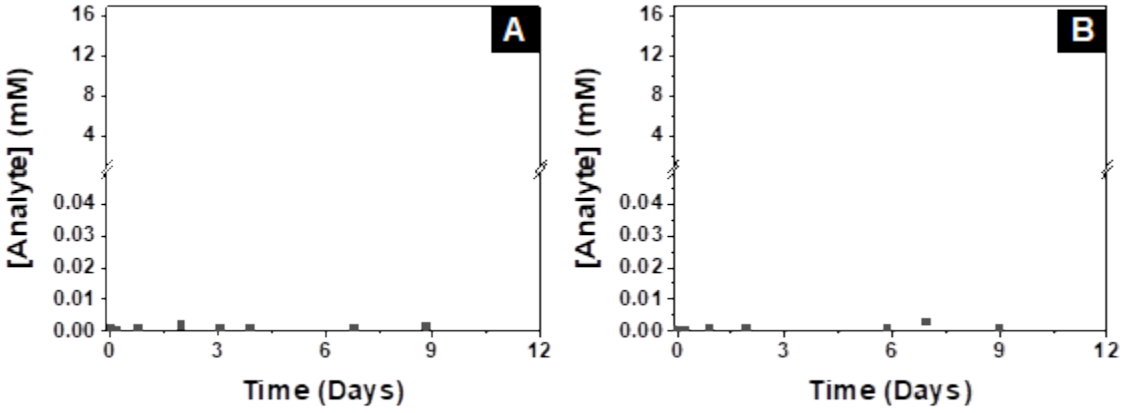

Figure S10. Control dissolution trials of UO_2 in ultra-pure water showing aqueous uranium concentration over time at (A) pH 8 and (B) pH 10.

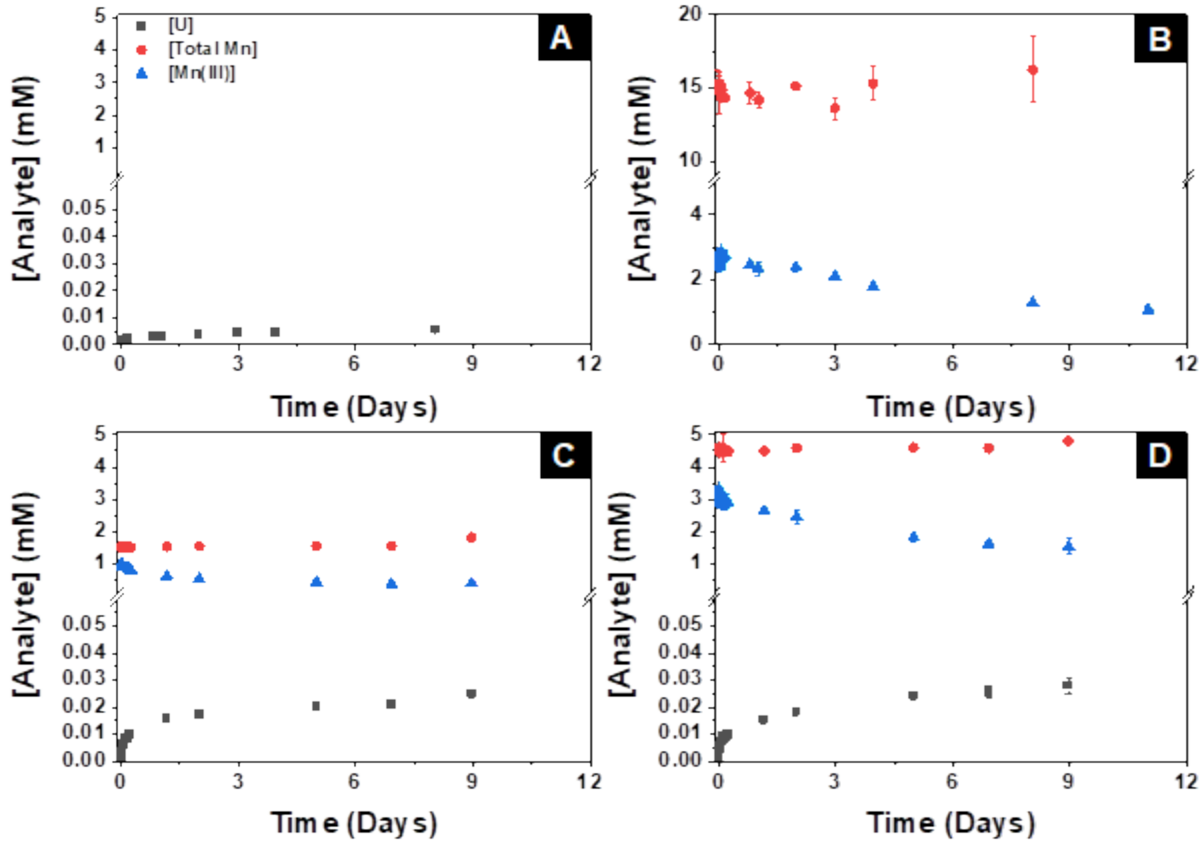

Figure S11. Dissolution trials at pH 8 of (A) UO_2 in 250 mM tartrate, (B) Mn(III)-tartrate in the absence of UO_2, (C) UO_2 in 1 mM Mn(III)-tartrate, and (D) UO_2 in 3 mM Mn(III)-tartrate.

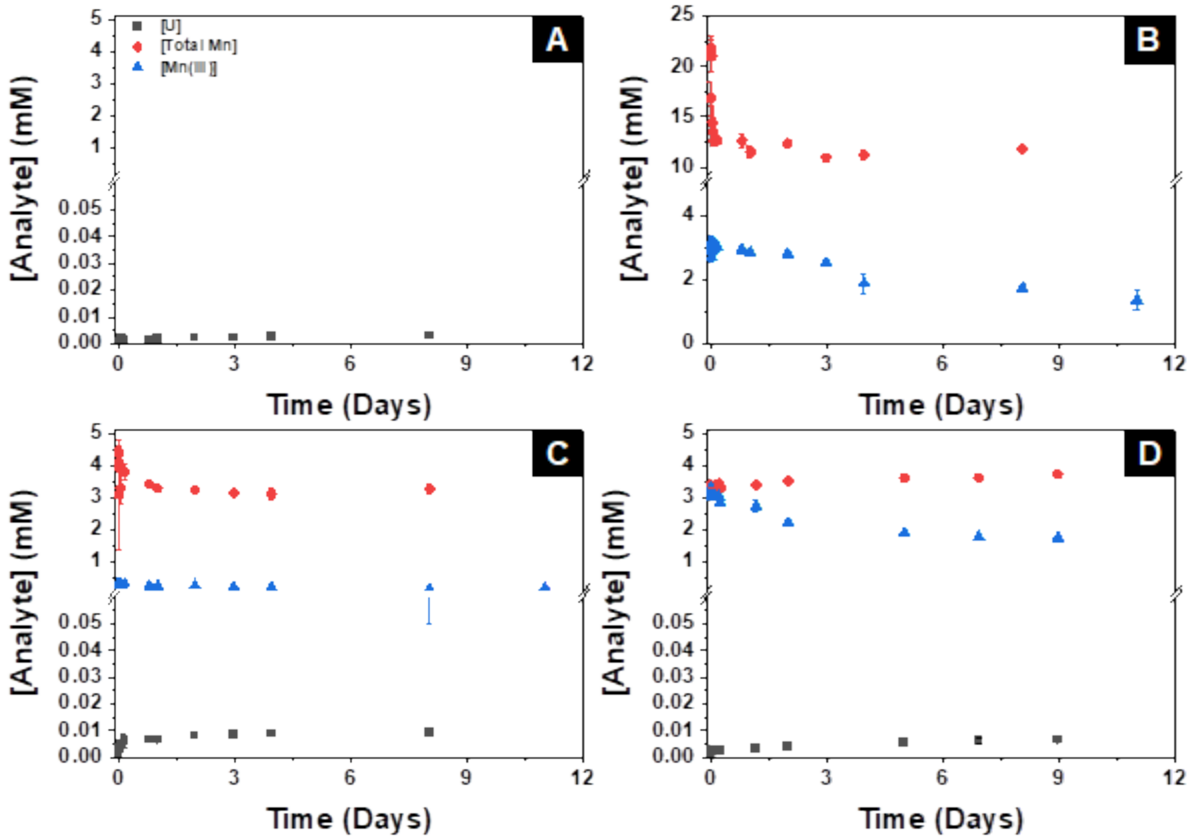

Figure 12. Dissolution trials at pH 10 of (A) UO_2 in 250 mM tartrate, (B) Mn(III)-tartrate in the absence of UO_2, (C) UO_2 in 1 mM Mn(III)-tartrate, and (D) UO_2 in 3 mM Mn(III)-tartrate.

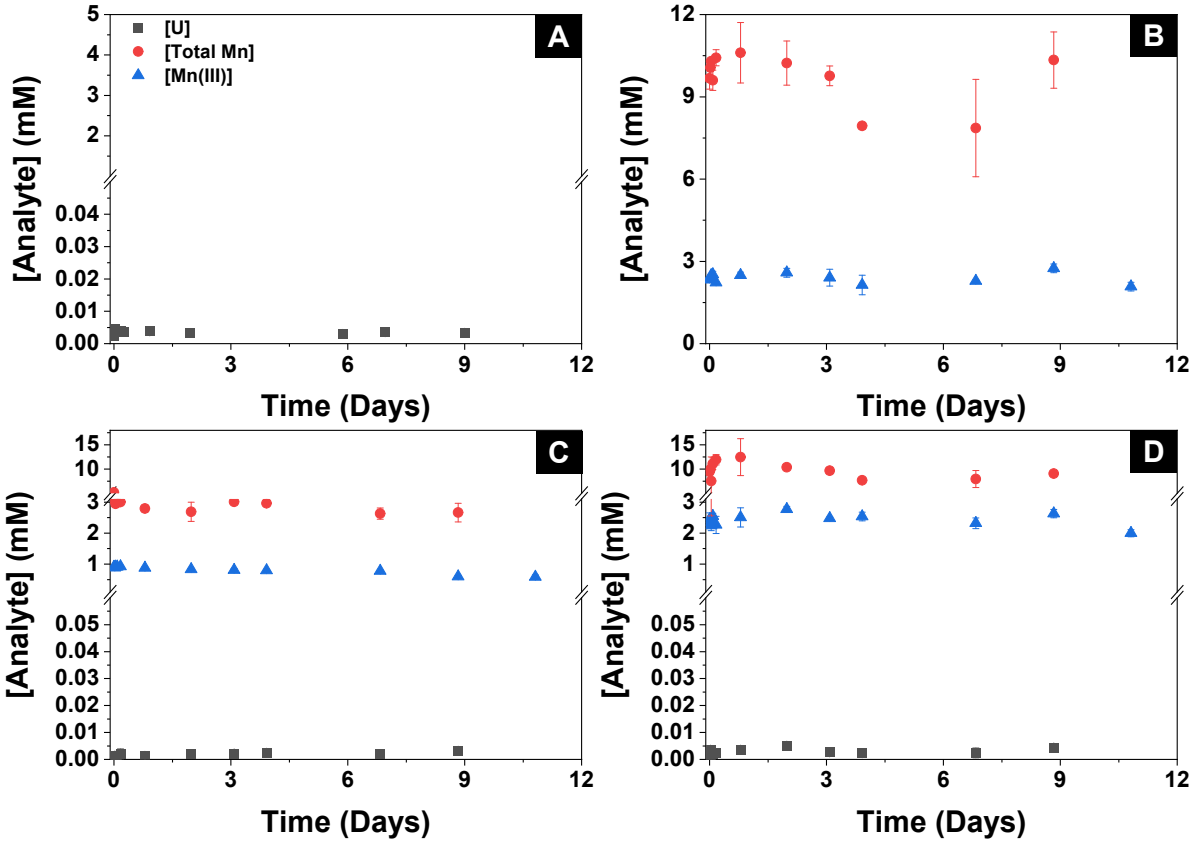

Figure 13. Dissolution trials at pH 8 of (A) UO_2 in 250 mM citrate, (B) Mn(III)-citrate in the absence of UO_2, (C) UO_2 in 1 mM Mn(III)-citrate, and (D) UO_2 in 3 mM Mn(III)-citrate.

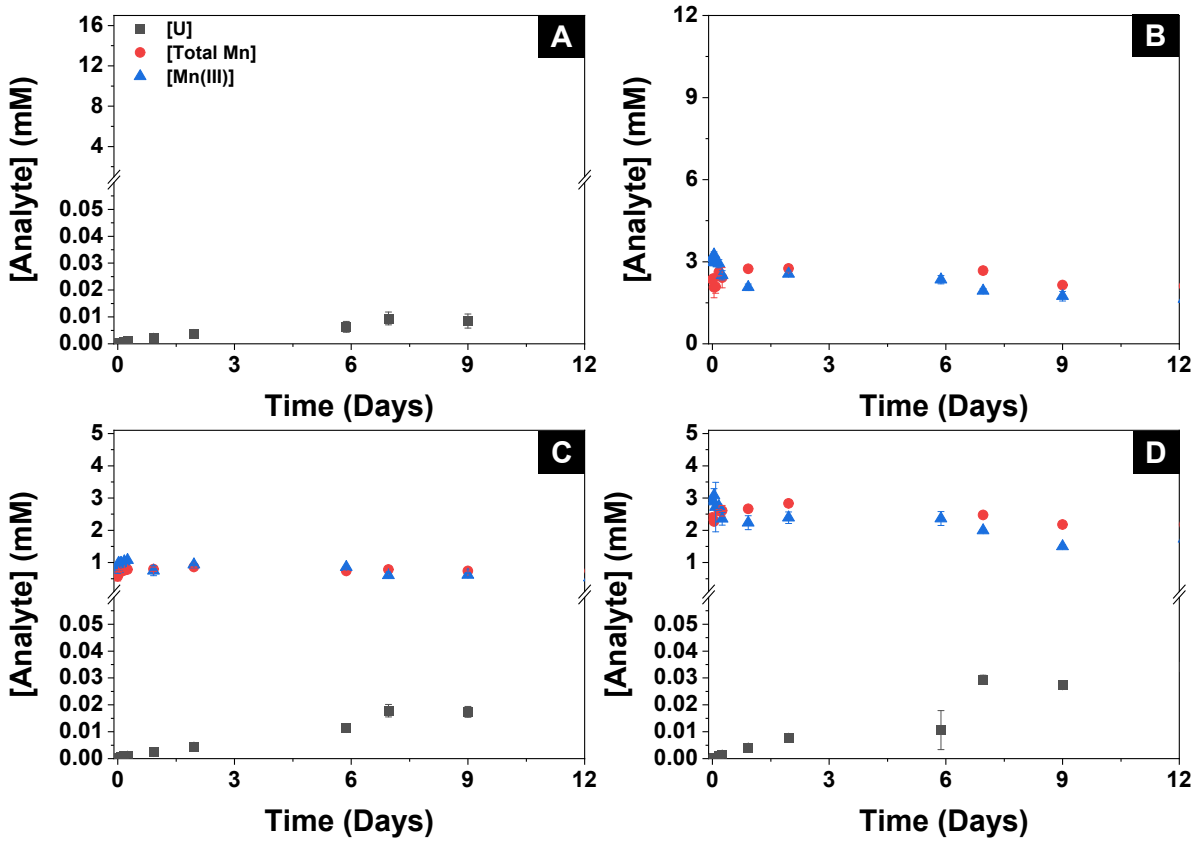

Figure 14. Dissolution trials at pH 10 of (A) UO_2 in 250 mM citrate, (B) Mn(III)-citrate in the absence of UO_2, (C) UO_2 in 1 mM Mn(III)-citrate, and (D) UO_2 in 3 mM Mn(III)-citrate.

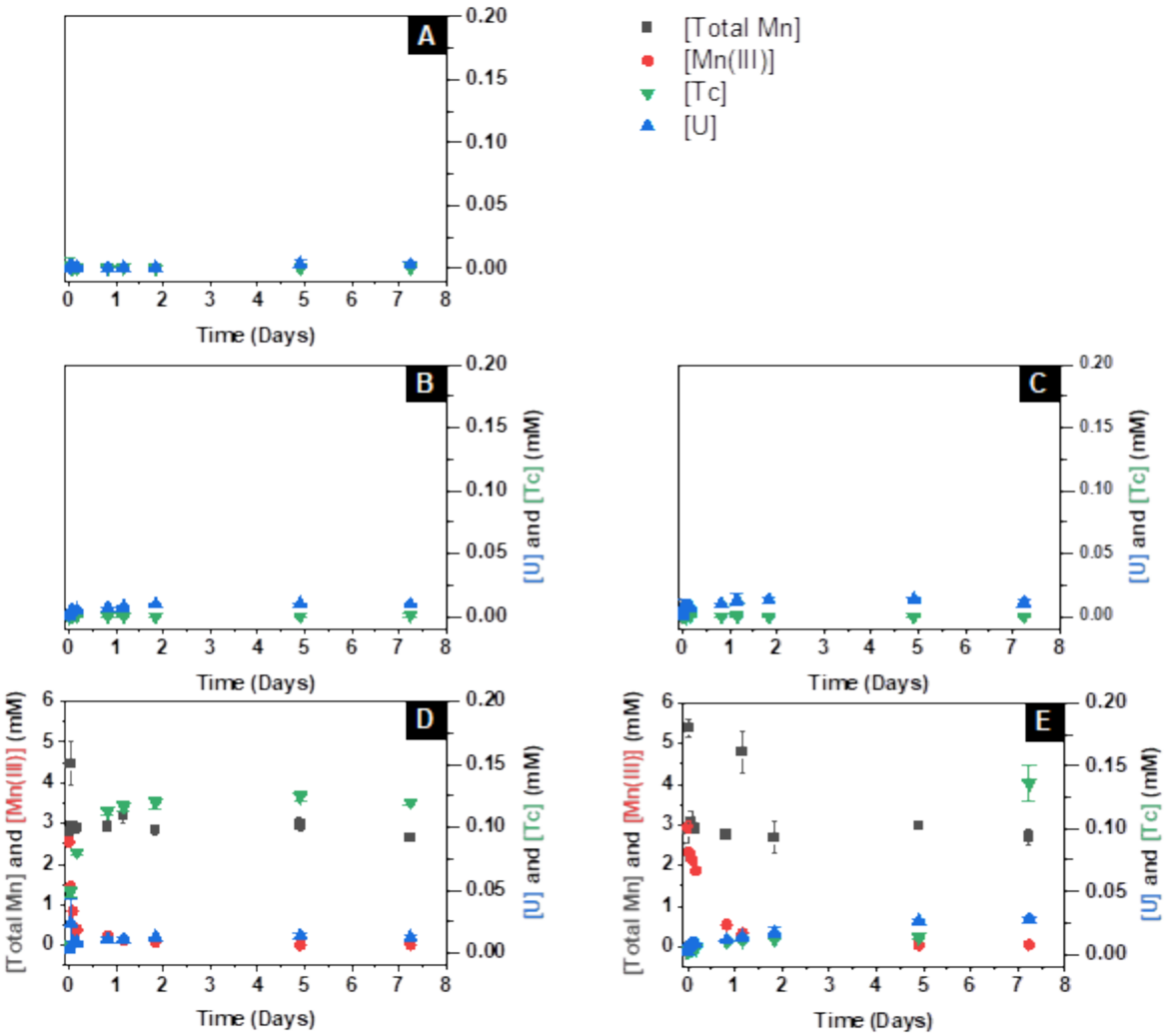

Figure 15. Dissolution trials of UO_2 and TcO_2 in (A) ultra-pure water, (B) 250 mM tartrate in the absence of manganese, (C) 250 mM citrate in the absence of manganese, (D) 3 mM Mn(III)-tartrate, and (E) 3 mM Mn(III)-citrate.

References

(1) Ram, R.; Charalambous, F.; Tardio, J.; Bhargava, S. *Characterisation of uraninite using X-ray diffraction (XRD) and general area detector diffraction system (GADDS)*; 2011.

(2) Ulrich, K.-U.; Singh, A.; Schofield, E. J.; Bargar, J. R.; Veeramani, H.; Sharp, J. O.; Bernier-Latmani, R.; Giammar, D. E. Dissolution of biogenic and synthetic UO2 under varied reducing conditions. *Environmental science & technology* **2008**, *42* (15), 5600-5606. DOI: 10.1021/es800647u PubMed.